19F Containment Ultimate Strength

19F.1 Introduction and Summary

This appendix describes analysis and judgement used to estimate the containment internal pressure capability and associated failure mode and location. The ultimate pressure capability of the containment structure is limited by the drywell head whose failure mode is plastic yield of the torispherical dome. The pressure capability is 1.025 MPa at 533 K (500°F) (typical temperature for most severe accident sequences), or 0.921 MPa at 644 K (700°F) [representative for those accidents in which the temperature exceeds 533 K (500°F)]. The containment is conservatively assumed to depressurize rapidly when the pressure capability is reached. No significant leakage through penetrations is anticipated before the capability pressure is reached. However, for the purpose of source term calculations, leakage in terms of leak areas is conservatively estimated for pressures below the capability pressure.

The primary function of the containment structure is to serve as the principal barrier to control potential fission product releases. The design basis event for this function is a postulated loss-of-coolant accident (LOCA). Based on this functional requirement, the containment pressure vessel is designed to withstand the maximum pressure and temperature conditions which would occur during a postulated LOCA. The ABWR containment system employs pressure suppression which allows a design pressure of 0.411 MPa and a design temperature of 444 K (340°F) for the primary containment pressure vessel. In addition the suppression pool retains fission products which could be released in the event of an accident. In this appendix the capability of the containment structural system of the ABWR standard plant to resist potentially higher internal pressures and temperatures associated with severe accidents is evaluated.

The primary containment vessel, also referred to as the RCCV for reinforced concrete containment vessel, is a right, cylindrical structure of the steel-lined, reinforced concrete design. The containment is integrated with the reactor building (RB) walls from the basemat up to the elevation of the containment top slab. The top slab, together with pool girders and building walls, form the spent fuel and equipment storage pools. The elevation view of the reactor building/containment structural system along 0°–180° direction is shown in Figure 19F-1. The containment is divided by the diaphragm floor and the reactor pressure vessel (RPV) pedestal into a drywell chamber and a suppression chamber. The drywell chamber above the diaphragm floor is called the upper drywell (U/D). The drywell chamber enclosed by the RPV support pedestal beneath the RPV is called the lower drywell (L/D). The primary containment and internal structures are shown in Figure 19F-2. The major penetrations in the containment wall include:

(1) The upper drywell equipment and personnel hatches at azimuth 130° and 230°

(2) The lower drywell equipment and personnel tunnels and hatches at azimuth 0° and 180°

(3) The suppression chamber airspace access hatch

(4) The main steam and feedwater pipe penetrations

Detailed descriptions of the containment design are included in Subsection 3.8.1.

The pressure boundary of the containment structure consists of the reinforced concrete containment vessel (RCCV) and the steel drywell head. The structural integrity of the RCCV is investigated for its global strength under internal pressure beyond the design basis using the FINEL computer program which is based on the nonlinear finite element method of analysis for axisymmetric reinforced concrete structures. The pressure capability of the steel drywell head is evaluated using approximate methods. During various severe accident conditions, the ABWR containment could also be challenged by high temperatures with a typical temperature of 533 K (500°F) for most accident sequences and a representative temperature of 644 K (700°F) for those accidents in which the temperature exceeds 533 K (500°F). At typical accident temperature of 533 K (500°F), the drywell head is found to have a ultimate pressure capability of 1.025 MPa and a service level C pressure capability of 0.77 MPa. For the RCCV the pressure capability at ambient temperature is governed by the top slab and its level C value (corresponding to ASME-III, Div. 2, CC-3420 and CC-3720 limits for factored load category) is 1.23 MPa. This is much higher than the ultimate pressure capability of the drywell head. On the basis of a recent Argone National Laboratory (ANL) study for the Sandia's 1/6-scale containment model, it is expected that with thermal effects included the RCCV pressure capability will not be reduced below the drywell head capacity for the range of temperatures considered. The drywell head is the controlling component for the structural strength of the containment structure.

In order to evaluate liner response to over- pressurization, liner plates are included in the FINEL analysis. The analysis results show that the liner strains are much smaller than the code allowables when the internal pressure is as high as 1.34 MPa. A separate evaluation further demonstrates that at the governing containment failure pressure of 1.025 MPa at 533 K (500°F), the liner and anchor system will maintain its structural integrity and no liner tearing will occur.

The leakage potential through large operable penetrations such as the drywell head, equipment hatches, and personnel airlocks is evaluated. Assuming no sealing action from degraded seals at temperatures above 533 K (500°F), the total leak areas before the capability pressure is reached are conservatively estimated to be:

Pressure	Leak Area	
MPa	Cm^2	In^2
0.100	0	0.00
0.412 (design)	0	0.00

Pressure	Leak Area	
MPa	Cm^2	In^2
0.460 (SIT)	0	0.00
0.512	7.94	1.23
0.584	17.9	2.77
0.653	27.8	4.31
0.722	37.7	5.85
0.790	47.6	7.39
0.860	57.6	8.93
0.929 (capability)	67.5	10.47

At and below the Structural Integrity Test (SIT) pressure of 0.460 MPa, leakage is within the design limit and the equivalent leak area is negligible.

In conclusion, the ultimate pressure capability is limited by the drywell head. The postulated failure mechanism is the plastic yield of the torispherical dome. The pressure capability is 1.025 MPa at 533 K (500°F), and it reduces to 0.929 MPa when the containment temperature reaches 644 K (700°F). The governing service level C (for steel portions not backed by concrete)/factored load category (for concrete portions including steel liner) pressure capability of the containment structure is 0.770 MPa at 533 K (500°F) which is the internal pressure required to cause the maximum stress intensity in the steel drywell head to reach general membrane yielding according to service level C limits of ASME-III, Division 1, Subsubarticle NE-3220.

The pressure capability evaluation described above is based on the deterministic approach. The uncertainties associated with the failure pressure are assessed in Attachment 19FA.

19F.2 RCCV Nonlinear Analysis

This subsection describes the non-linear analysis performed for the reinforced concrete containment vessel (RCCV) (excluding the drywell head) of the ABWR Standard Plant. Computer code “FINEL” was used for evaluation of the axisymmetrical components of the RCCV.

19F.2.1 Finite Element (FE) Model Description

The containment and the containment internal structures are axisymmetric while the RCCV top slab together with the reinforced concrete girders even though not axisymmetric, are idealized and included in the axisymmetrical model. Solid elements are used to represent the girders at the top of the RCCV, approximating the stiffness of the actual structure.

For simplicity, the reactor pressure vessel (RPV), the reactor building outside of the RCCV and superstructure above the operating floor, are not modeled. To represent the restraining effects of the floors outside the containment, horizontal restraining elements are used with pseudo material properties. The model includes concrete elements, the reinforcing steel, the steel liner plate of the drywell, and the wetwell and the diaphragm floor structures, and the structural steel elements used for the pedestal.

The model consists of 868 nodal points and 1280 elements. There are 448 elements used with unidirectional stiffness representing rebar, whereas 832 elements are isotropic, representing steel, concrete, and soil. The soil below the foundation mat was modeled to a depth of 50.0m and to a radius of 76.0m. See Figure 19F-3 for the model.

The FINEL computer program permits the specification of bi-linear, brittle or ductile material properties. The concrete and soil elements are specified to have brittle properties such that they are strong in compression and weak in tension. The steel plate elements and the rebar elements are specified to have ductile material properties with the same strength in tension and compression. The capability of the FINEL program to accommodate ductile and brittle material behaviors permits both concrete cracking and yielding of steel and rebar. This allows the program to consider redistribution of forces throughout the structure due to the non-linear behavior.

19F.2.2 Analysis

The FE model was run for three different load conditions shown in Table 19F-1.

(1) Structural Integrity Test 1 (SIT-1), with 0.46 MPa pressure in the drywell and wetwell (RCCV).

(2) Structural Integrity Test 2 (SIT-2), with 0.411 MPa pressure in the drywell and 0.18 MPa in the wetwell.

(3) Four times design pressure, with 1.34 MPa pressure in the RCCV.

Since FINEL performs non-linear analysis, it is necessary to apply simultaneously all loads of a loading combination. The program utilizes a stepwise linear iteration technique. The first cycle results are for elastic analysis. Based upon results of the first cycle, stiffness of all elements are adjusted by the program prior to the next iteration cycle.

19F.2.3 Results

Table 19F-1 summarizes analytical results for various loading conditions. The results are shown in terms of maximum rebar stresses, concrete stresses, liner strains and structural deformations.

Based on the FINEL analysis, it can be concluded that the axisymmetric components of the RCCV, as designed based on ASME Section III Division 2 code requirements, can withstand an internal pressure of 1.34 MPa i.e, four times the design pressure, with stresses and strains in the rebar, liner plate and concrete within code allowable limits. The strength is governed by wetwell wall. The strength of the non-axisymmetric top slab region is evaluated by extrapolation of the elastic analysis results using a 3D finite element model as discussed in Subsection 19F.3.1.1.

19F.3 Prediction of Containment Ultimate Strength

19F.3.1 Structural Capability

19F.3.1.1 Concrete Shell

The structural integrity of the RCCV axisymmetric components has been demonstrated for an internal pressure of 1.34 MPa from the FINEL analysis. Based on extrapolation of analysis results, estimate of the level C pressure capability and the ultimate pressure capability is made and discussed in this subsection. The level C pressure capability is defined to be the pressure value at which the ASME-III, Div. 2, CC-3420 and CC-3720 limits for factored load category are reached. The ultimate pressure capability is assumed reached when rebars at both faces of a cross section reaching yield stress. The estimated pressure capabilities of the various components of the RCCV are shown in Table 19F-2. It should be noted that the extrapolation of results gives only approximate values beyond the analyzed values. The level C pressure value of 1.23 MPa for the top slab shown in Table 19F-2 is based on extrapolation of elastic 3D STRARDYNE analysis results and it is governed by the strength of the supporting pool girders. It should be recognized that this value could be somewhat different from inelastic analysis results. The ultimate pressure capability of the top slab is not made since its level C value is much higher than the drywell head ultimate pressure discussed in Subsection 19F.3.1.2.

The analysis performed was static analysis. Dynamic effect on structural response becomes significant only when the rate of applied loading is within the range of natural periods of the structure. The fundamental natural period of the integrated RB and RCCV structures is less than one second. Therefore, containment loading resulting from severe accident conditions can be treated statically when the rate of loading buildup is longer than one second. For all accidents sequences considered in this PRA, except hydrogen detonation, the pressure buildup rate within the containment is longer than one second. Thus, the results based on static analysis can be applied. Since the ABWR containment is inerted, hydrogen detonation is of no concern.

During various severe accident conditions, the ABWR containment could be challenged by high temperatures with a typical temperature about 533 K (500°F). The effect of elevated temperature on containment pressure capability has been investigated recently by Argonne National Laboratory (ANL) (Reference 19F-1). The ANL study concluded that for temperatures up to 644 K (700°F), the failure mode and location did not change from the case of internal pressure alone, and the failure pressure was reduced slightly (11% maximum) from that predicted for the internal pressure alone case. On the basis of the ANL study it is expected that with thermal effects included the RCCV pressure capability will be not reduced below the drywell head capability for the range of temperatures considered.

19F.3.1.2 Drywell Head

This subsection presents an evaluation of the structural capability of the drywell head under internal pressure and temperature loading. The leakage potential of the head closure is discussed in Subsection 19F.3.2.2.

The drywell head which covers the 10.29 m (33 ft-9 in.) in diameter opening in the upper drywell top slab is a steel torispherical dome assembly. Figure 19F-4 shows the major dimensions of the design. Under internal pressure loading, the most critical location of this type of configuration is the knuckle (or torus) region of the torispherical dome which may fail by plastic yield or buckling.

For torispherical pressure vessel heads, an approximate formula for the limit pressure at which significant plastic deformation occurs was developed by Shield and Drucker (Reference 19F-2) based on the upper and lower bound theorems of limit analysis, and it is

$$P_c = S_y\left\{(0.33 + 5.5r/D)\frac{t}{L} + 28(1-2.2r/D)\left(\frac{t}{L}\right)^2 - 0.0006\right\} \qquad (19F\text{-}1)$$

where:

P_c = limit pressure

S_y = yield strength of the material

t = uniform thickness of the head

r = radius of the knuckle shell

D = diameter of the cylindrical shell

L = radius of the spherical cap

Substituting the dimensions shown in Figure 19F-4 into Equation 19F-1 gives

$$P_c = 0.003965 \cdot S_y$$

The material yield strength depends on temperature. The actual strength of as-built material is generally higher than the specified minimum value used in design. To have a more realistic estimate of the structural strength, the minimum yield strength of material SA-516, Gr. 70 as specified in Appendix I of ASME Section III is increased by 10%. The calculated limit pressure as a function of temperature is shown in Figure 19F-5. As shown in the figure, the limit pressure is 1.025 MPa at 533 K (500°F), and reduces to 0.929 MPa at 644 K (700°F) which is a representative temperature for those accidents in which the temperature exceeds 533 K (500°F). From a linear elastic finite element analysis, it is found that a pressure of 0.770 MPa at 533 K (500°F) is required to cause the maximum stress intensity in the head to reach general membrane yielding according to service level C limits of ASME-III, Division 1, Subsubarticle NE-3220.

Buckling is another potential failure mode of the torispherical head under internal pressure since the knuckle is subjected to compressive stress in the hoop direction. Galletly recently (Reference 19F-3) proposed a design equation for preventing buckling in fabricated torispherical shells under internal pressure.

$$P_d = \frac{80 S_y \left(\frac{r}{D}\right)^{0.825}}{\left(\frac{D}{t}\right)^{1.5} \left(\frac{L}{D}\right)^{1.15}} \qquad (19F\text{-}2)$$

This equation is based on his previous studies (References 19F-4 and 19F-5) and is formulated for design use with knock-down (capacity reduction) factors included. As compared to all known test results (43 in total), the ratios of the actual buckling pressure to the allowable buckling pressure predicted by this equation were found to range from 1.51 to 4.01. Hence, a minimum factor of safety of 1.5 is ensured by this equation.

The test data presented in Reference 19F-3 (excluding the test performed by Blenkin since no buckling was observed at the maximum test pressure) are summarized graphically in Figure 19F-6, showing the relationship between the test and predicted pressures. The predicted pressures, as can be seen, are at least 1.5 times lower than the test results. In order to gain more insight about the data variability, statistical analyses are performed and the results are given in Figure 19F-7. The PDF (probability density function) of the data shown by solid lines is the histogram of 42 data points expressed in terms of the ratio of test to predicted pressure. It is observed that the data can be reasonably approximated by the lognormal distribution. The medium value of the test to predicted pressure ratios in the data set is 2.27 and the logarithmic standard deviation is 0.293. The resulting lognormal density and cumulative functions are shown in Figure 19F-7. The cumulative probability is 8% for the ratio up to 1.5. It means that the probability of the ratio of actual to predicted pressure being less than 1.5 is 8%. In other

words, there is 92% confidence that the margin of safety against buckling is at least 1.5 when Equation 19F-2 is used. The 1.5 factor of safety corresponding to 92th percentile is deemed sufficient for the assurance of no buckling failure against severe accident loadings of very low probabilities of occurrence. Equation 19F-2 can be therefore used for the determination of level C buckling pressure of torispherical heads.

Substituting the dimensions shown in Figure 19F-4 and the material properties specified in Appendix I of ASME Section III for SA516, Gr. 70 into Equation 19F-2, the level C buckling pressure for the ABWR drywell head is calculated to be 0.860 MPa at 533 K (500°F). It is higher than 0.770 MPa associated with general membrane yielding per level C stress intensity limits. Therefore, the governing level C pressure is 0.770 MPa.

As mentioned earlier, Equation 19F-2 has a factor of safety of 1.5 as compared to the lower bound of all known test results. From a statistical study of these test results, the medium buckling pressure is estimated to be 2.27 times the value predicted by Equation 19F-2. Subsequently, the critical buckling pressure of the ABWR drywell head are:

Lower bound = 1.5 x 0.860 MPa = 1.246 MPa,

Best estimate = 2.27 x 0.860 MPa = 1.839 MPa.

A comparison with the plastic yield limit pressure P_c calculated above indicates that plastic yield will occur before buckling and is the governing failure mode of the drywell head. The capability pressure is 1.025 MPa at 533 K (500°F), and reduces to 0.929 MPa when the containment temperature reaches 644 K (700°F).

19F.3.2 Leakage Potential

The previous subsection has addressed the structural capability of the containment structures under severe accident conditions. However, the containment function can be compromised if excessive leakage occurs before the capability pressure is reached. Leakage above the design allowable could result from failure of the liner plate and penetrations at high pressures and temperatures. The leakage potential of the liner plate and penetrations is evaluated in the following subsections.

19F.3.2.1 Liner Plate

As discussed earlier, the containment liner plates were included in the FINEL model. The maximum liner strains are found to be well within the code allowables when the internal pressure is as high as 1.34 MPa. Therefore, liner tearing is not expected to occur before the capability pressure of the drywell head is reached. This is confirmed by a separate evaluation as follows.

The ABWR containment liner plate system consists of 6.35-mm (1/4-in) thick plate made of ASME SA-516 Grade 70 steel. The liner plate is anchored into the concrete containment

through WT 4 X 7.5 made of ASTM A-36 steel and welded to the liner plate. The following are the pertinent data of the ABWR containment liner plate system used for the evaluation.

- Concrete Containment:

  Inside Radius = 14.5 m (571 in)

  Thickness = 2.0 m (78.7 in)

  Hoop Rebar = 4.57 cm^2/cm (1.8 in^2/in) total on both faces

  Vertical Rebar = 7.05 cm^2/cm (1.666 in^2/in) total on both faces

- Steel Liner Plate:

  6.35-mm (1/4-in) thick ASME SA 516 Grade 70

  Yield stress at 294 K (70°F) = 262 MPa

  Yield stress at 533 K (500°F) = 212 MPa

  Ultimate Uniaxial Strain at Fracture = 21%

  [Based on ASTM 516 Grade 70 minimum guaranteed elongation in 51 mm (2")]

- Liner Anchor:

  WT 4 X 7.5 spaced at 500 mm on center

  Yield stress at 294 K (70°F) = 248 MPa (A36 steel)

The following severe accident conditions are used for the evaluation of the ABWR containment liner plate.

- Containment Internal Pressure = 1.025 MPa
- Steam Jet Temperature = 533 K (500°F)
- Ambient Temperature = 311 K (100°F)
- Rise in Temperature = 477 K (400°F)

Due to the internal pressure, the liner plate has a tendency to elongate by virtue of hoop tension whereas it has a tendency to shorten due to compression on the inside face of the containment for elevated internal temperature. Thus, the combination of internal pressure and temperature loads on the liner plate has compensatory effects. The friction and the physical bond between the liner plate and concrete wall are conservatively neglected for the evaluation. The

corresponding shrinkage strains, being small, are neglected, and the concrete is assumed to have zero tensile strength.

(1) Evaluation for Internal Pressure Loading

The hoop force due to the internal pressure of 1.025 MPa on an internal radius of 14.5 m (571 in) is computed to be 13690 kg/cm (76.5 kips per inch) height of the containment. Assuming that this hoop force is resisted by the total hoop steel of 11.6 cm^2 (1.8 in^2) and liner plate area of 1.61 cm^2/cm (0.25 in^2 per inch) height of the containment, the hoop stress is computed to be 257 MPa which gives the value of hoop strain of 0.13%.

This compares very closely with the strain values obtained from the "FINEL" analysis for 1.025 MPa internal pressure which gave maximum strain of 0.126%. Assuming a very conservative estimate of strain concentration factor of 33 at the discontinuities on the Sandia Containment Test results based on internal pressure of 1.11 MPa (Reference 19F-6), the maximum liner plate strain due to the internal pressure is estimated to be 0.13 X 33 = 4.3%. This strain is still far lower (by a factor of almost 5) than the ultimate fracture strain of 21% for the liner plate material. The internal pressure results in uniform tension in the liner but does not produce any load on the liner anchors. Thus, it can be inferred that the liner plate will not tear for the severe accident pressure of 1.025 MPa.

(2) Evaluation for Thermal Loading/Jet Impingement

The internal temperature causes compressive forces on the liner resulting in potential buckling of the plate, as illustrated in Figure 19F-8. The thermal strain resulting from a 477 K (400°F) temperature rise is 0.002744 cm/cm (0.002744 in/in). The resulting hoop membrane force for the 6.35-mm (1/4-in) thick liner plate is 4625 kN/m (26.4 k/in). This is beyond the elastic limit and a plastic solution is sought using the procedure suggested in Bechtel Topic Report BC-TOP-1 (Reference 19F-7). For the buckled configuration shown in Figure 19F-8, the following spring constants are found:

K_c = 890 kN/m/m (200 k/in/in) for the anchor

K_{BPL} = 441 kN/m/m (99 k/in/in) for the bent plate

K_{RPL} = 1522 kN/m/m (342 k/in/in) for plate relaxation

The resulting total force N_T on the system is found to be 6244 kN/m (35.64 k/in) and the corresponding deflection δ is 1.9 mm (0.0748 in). From the energy balance approach, the safety factor expressed in terms of the ratio of the total energy capacity of the anchor to the energy required for the equilibrium is calculated to be 1.9. The forces exerted on the liner plate and anchor are 897 kN/m (5.12 k/in) and 865 kN/m

(4.94 k/in) which are within their respective yielding capacity of 1356 kN/m (7.74 k/in) and 929 kN/m (5.3 k/in). Therefore, the anchor system is safe under applied loads.

(3) Conclusions

Based on the above discussions it is concluded that the ABWR containment liner plate and the liner anchorage will maintain its structural integrity even when subjected to severe accident pressure of 1.025 MPa at 533 K (500°F). In this evaluation, a very conservative strain concentration factor of 33, observed at the discontinuities in the Sandia containment tests, has been used. It is demonstrated that there are adequate margins over the maximum conceivable strains to the ultimate fracture strains available to preclude the type of tearing failures observed in the Sandia containment tests. It should also be noted that there are major differences between the liner plate system used in the Sandia tests and the ABWR containment. The significant difference is the use of intermittent stud type liner anchor in the Sandia tests as opposed to the welded WT 4 anchors for the ABWR containment. This should result in a more uniform distribution of the strain for the ABWR containment and in much lower strain concentration factors compared to those observed in the Sandia test. This will further improve the margins of safety over the ones computed.

19F.3.2.2 Penetrations

An ANL study (Reference 19F-8) assigned high priority to the study of large operable penetrations such as the drywell head closure, equipment hatches, and personnel airlocks since they are expected to have high potential for leakage under severe accident conditions. Leakage from fixed penetrations (both electrical and mechanical) appears to be less likely based on the results of experiments conducted to date by Sandia National Labratories (SNL) and its contractors (Reference 19F-8). In fact, according to the same reference, no leakage was detected from any of the three current electrical penetration assemblies (EPAs) during the severe accident testing (steam environments). Depending on the EPA type the highest temperature loading ranged from 456 K (361°F) to 644 K (700°F), and the highest pressure loading ranged from 0.517 MPa to 1.069 MPa. The EPAs used in the ABWR containment will be capable of maintaining leak tightness up to the containment pressure of 1.025 MPag and temperature of 644 K (700°F)(Subsection 8.3.3.7). The leakage estimate in this study therefore concentrates on large operable penetrations.

The leakage potential of operable penetrations depends on both the relative position of the sealing surfaces and the performance of the seal material. The position of the sealing surfaces depends on the initial conditions (metal-to-metal contact is maintained under design conditions for most penetrations) and on the deformations induced by accident pressure and temperature. The seal performance depends mainly on temperature as well as the effect of thermal and

radiation aging. The recent SNL tests of seals for mechanical penetrations, Reference 19F-8, indicated that

(1) In a steam environment at a constant pressure of 1.069 MPa, the mean degradation temperature was 544 K (520°F) for silicon rubber and 606 K (630°F) for ethylene proplylene rubber (EPR), and

(2) In a nitrogen environment at a constant pressure of 1.069 MPa, the mean degradation temperature was 528 K (490°F) for neoprene, and

(3) The degradation temperature was not significantly affected by thermal and radiation aging.

Neoprene is not used for operable penetrations in the ABWR containment and the seal degradation temperature is conservatively assumed to be 533 K (500°F). The SNL study also showed that even a degraded seal can prevent leakage if the separation of the sealing surfaces is small [less than 0.127 mm (0.005 in.)].

Sandia (Reference 19F-8) has proposed the following equations for "available gasket springback", S_p, for evaluating the leakage potential as a function of the compression set retention and the degradation temperature:

$$S_p = (1 - C_B)S_q h_i \text{ for} (T < T_d) \quad (19F\text{-}3)$$

$$S_p = 0.127 \text{mm} (0.005 \text{ inch}) \text{for} (T > T_d) \quad (19F\text{-}4)$$

where:

C_B = the compression set retention (a dimensionless measure of the permanent set in the gasket caused by aging),

S_q = the squeeze as illustrated in Figure 19F-9 (a dimensionless measure of the gasket deformation under normal operation conditions),

h_i = the initial seal height, and

T_d = the degradation temperature of the gasket material.

Equation 19F-3 is based on the assumption that significant leakage can be prevented as long as positive compression of the gasket is maintained. Equation 19F-4 is empirical based on test results that even a degraded gasket can effectively prevent leakage if the separation of the sealing surfaces is equal to or less than 0.127 mm (0.005 in).

For the pressure-unseating drywell head closure and equipment hatches, the pressure required to separate the sealing surfaces is a function of the bolt preload, axial stiffness of the bolts and the compression flanges, and the differential thermal expansion between the bolts and the compression flanges. The separation pressure for operable penetrations typically ranges from 1.1 to 1.5 times design pressure (Reference 19F-8). In this study, the separation pressure is conservatively assumed to be 0.460 MPa which is the Structural Integrity Test (SIT) pressure (1.15 times design pressure). At and below this pressure, a metal-to-metal contact is maintained and no leakage other than design allowable leak rate is anticipated, even if the seal degradation temperature of about 533 K (500°F) has reached. Additional pressure in excess of the separation pressure is carried entirely by the bolts. The separation displacement between the sealing surface after the separation pressure is reached is:

$$s = \frac{\pi r^2 (p - p_s)}{K_b} \qquad (19F\text{-}5)$$

where:

r = the inside radius of the equipment hatch sleeve or drywell head,

p_s = the separation pressure, and

K_b = the total bolt axial stiffness.

The above expression neglects the flexibility due to axial deflection of the compression flanges caused by the Poisson effect which contributes little to the total flexibility of the bolts. This approach for predicting leakage is based on the consideration of structural deformations in terms of separation of connecting flanges of pressure unseating equipment hatches and drywell head. The adequacy of this approach has been recently confirmed by the Sandia hatch leakage tests (Reference 19F-9) in that the predicted leakage onset pressures were in favorable agreement with the test results. The drywell head anchorage to the top slab has a pressure capability higher than the drywell head shell and the leakage path of the drywell head assembly before the failure pressure is reached is through the flanges.

The drywell head is a 10.3-m diameter closure with double seal. One hundred twenty 68-mm diameter bolts hold the head in place. There are 3 equipment hatches in the containment wall. The largest of them has twenty 36-mm diameter bolts with double seal, and has a diameter of 2.6 m. According to Equation 19F-5, the separation displacement at 0.929 MPa capability pressure is calculated to be about 0.0838 mm (0.0033 in) for the drywell head and 0.140 mm (0.0055 in) for the most flexible equipment hatch. The equipment hatch separation displacement is slightly larger than 0.127 mm (0.005 in). However, the resulting gap of 0.0127 mm (0.0005 in.) is small and no significant leakage is expected before the capability pressure is reached.

For equipment hatches, another potential leakage mechanism is ovalization of the sleeve which causes the sleeve to slide relative to the tensioning ring (or the cover flange). An initiation of leakage due to sleeve ovalization, however, requires significant deformations of the containment shell around the equipment hatch. The average circumferential membrane strain in the shell that is needed to result in the initiation of leakage from ovalization for equipment hatches identified in the ANL survey (Reference 19F-8) was found to range from 2.5% to 7.3% by SNL (Reference 19F-8). For the equipment hatches under consideration, the ovalization leakage onset strain which is the ratio of the sleeve wall thickness at the sealing surface to the sleeve radius ranges from about 1.2% to 5.8%. At a pressure of 1.34 MPa, the maximum radial deflection of the wetwell wall was calculated to be 25.0 mm (0.983 in.) from the FINEL analysis (Table 19F-1). The corresponding hoop membrane strain is 0.15%. It is less than 1.2% and no leakage from sleeve ovalization of the equipment hatches will occur before the capability pressure is reached.

The leakage rate which should be small for the separation displacements of the drywell head and equipment hatches defined above cannot be quantified based on current capabilities. To facilitate source term calculations, leak areas as a function of pressure are conservatively taken to be the product of the separation displacements and the seal length for the drywell head and equipment hatches. It should be noted that this approach results in a very conservative leak area estimate since

(1) the seal is assumed lost at 533 K (500°F), and

(2) no credit is taken for the springback capability of 0.127 mm (0.005 in.) for degraded seals.

The personnel airlocks are the pressure-seating type. Although separation between the sealing surfaces at the door corners may still be possible at high pressures, the amount of separation is nevertheless expected to be less than that of the pressure-unseating drywell head and equipment hatches at same pressures. Therefore, no calculations are made to predict separation displacements for the airlocks. Instead, the leak area through the airlocks is assumed to be 10% of the sum of the leak areas estimated for the drywell head and equipment hatches. This assumption is realistic since the sealing length of the airlocks is less than 20% of the total sealing length of the drywell head and equipment hatches, and the separation of airlock sealing surfaces is expected to be smaller.

The total estimate of pressure-dependent leak areas attributed to the drywell head, equipment hatches and personnel airlocks is shown below. At and below the separation pressure [0.460 MPa], leakage is within the design limit and the equivalent leak area is negligible.

Pressure	Leak Area	
MPa	Cm^2	In^2
0.100	0	0.00
0.411	0	0.00
0.460	0	0.00
0.515	7.93	1.23
0.584	17.9	2.77
0.653	27.8	4.31
0.72	37.7	5.85
0.791	47.6	7.39
0.860	57.6	8.93
0.929	67.5	10.47

19F.3.3 Summary

The ultimate pressure capability of the containment structure is limited by the drywell head whose failure mode is plastic yield of the torispherical dome. The pressure capability is 1.025 MPa at 533 K (500°F) and reduces to 0.929 MPa at 644 K (700°F). The governing service level C (for steel portions not backed by concrete)/factored load category (for concrete portions including steel liner) pressure capability of the containment structure is 0.770 MPa at 533 K (500°F) which is the internal pressure required to cause the maximum stress intensity in the steel drywell head to reach general membrane yielding according to service level C limits of ASME-III, Division 1, Subsubarticle NE-3220.

No liner leakage will occur before the capability pressure is reached. Leakage through fixed (mechanical and electrical) penetrations is negligible compared to leakage through large operable penetrations such as the drywell head, equipment hatches, and personnel airlocks. The total pressure-dependent leak areas attributed to those operable penetrations are conservatively estimated in Subsection 19F.3.2.2, assuming no sealing action from degraded seals at temperatures above 533 K (500°F).

19F.4 References

19F-1 Pfeiffer, P. A., Kennedy, J. M., and Marchertas, A. H., "Thermal Effects in Concrete Containment Analysis", Fourth Containment Integrity Workshop, June 15-17, 1988.

19F-2 Shield, R. T., and Drucker, D. C., "Design of Thin-Walled Torispherical and Toriconical Pressure-Vessel Heads", Journal of Applied Mechanics, Transaction of ASME, June 1961.

19F-3 Galletly, G.D., "A Simple Design Equation for Preventing Buckling in Fabricated Torispherical Shells under Internal Pressure", ASME Journal of Pressure Vessel Technology, Vol. 108, November 1986.

19F-4 Galletly, G. D., and Radhamohan, S. K., "Elastic-Plastic Buckling of Internally-Pressurized Thin Torispherical Shells", Journal of Pressure Vessel Technology, ASME, Vol. 101, August 1979.

19F-5 Galletly, G.D., and Blachnut, J., "Torispherical Shells Under Internal Pressure - Failure Due to Asymmetric Plastic Buckling or Axisymmetric Yielding", Proc. of Institution of Mech. Engineers, Vol. 199, No. C3, 1985.

19F-6 Clauss, D.B., "Round Robin Analysis of the Behavior of a 1:6 scale reinforced concrete containment model pressurized to Failure: Post-test Evaluations", NUREG/CR-5341 SAND 89-0349, Sandia National Laboratories, October 1989.

19F-7 "Containment Building Liner Plate Design Report", BC-TOP-1, Rev. 1, Bechtel, December 1972.

19F-8 Clauss, D. B., von Riesemann, W. A., and Parks, M. B., "Containment Penetrations", SAND88-0331C.

19F-9 Parks, M.B., Walther, H.P., and Lambert, L.D., "Evaluation of the Leakage Behavior of Pressure-Unseating Equipment Hatches and Drywell Heads", SAND90-180C, 18th Water Reactor Safety Meeting, October 1990.

Table 19F-1 Summary of Stresses and Strains

Loading Case				Maximum Rebar Stress/ Allow. Stress		Liner Strain		Concrete Comp. Stress/ Allow. Str (MPa)	Component Rebar Stresses / Allowable Stresses (MPa)								Max. Radial Defl. @ Wet-well mm (In.)
									Wetwell		Drywell		Basemat		Diaphrg.		
No.	Title	P.D. MPa	P.W. MPa	Merid. MPa	Hoop MPa	Tens. mm/mm	Comp. mm/mm		Mer.	Hoop	Mer.	Hoop	Rad.	Hoop	Rad.	Hoop	
1	SIT-1	0.359	0.359	79.3 310.3	82.7 310.3	.00052	–.00011	–3.86 –16.55	79.3 310.3	82.7 310.3	42.7 310.3	35.2 310.3	27.6 310.3	30.3 310.3	75.2 310.3	42.7 310.3	6.25 (.246)
2	SIT-2	0.310	0.138	60.7 310.8	31.0 310.8	.00035	–.00007	–3.86 –16.55	41.6 310.3	31.0 310.3	20.0 310.3	22.8 310.3	26.2 310.3	27.6 310.3	60.7 310.3	26.2 310.3	2.29 (.090)
3	4Pa.	1.24	1.24	277.9 413.7	337.8 413.7	.00185	–.00016	–4.69 –23.4	277.9 413.7	337.8 413.7	200.6 413.7	93.8 413.7	84.1 413.7	74.5 413.7	230.3 413.7	128.2 413.7	24.9 (.983)

Table 19F-2 Summary of Pressure Capabilities of Various Components of the RCCV

Structural Component	Pressure Capability MPa Categories (Criteria) Level C MPa	Ultimate** MPa
Wetwell	1.467	1.818
Upper Drywell	2.404	>2.659
Basemat	4.500	6.203
Top Slab*	1.232	- - -

Notes:

* The pressure capability shown for the RCCV top slab which is a non-axisymmetric portion of the RCCV, is calculated based on extrapolation of elastic STARDYNE analysis results. Pressure value 1.232 MPa is governed by the pool girders, pressure capacity of the reinforcing of the top slab is 1.329 MPa.

** Ultimate capability has been calculated based on rebars at both faces of a cross section reaching yield stress.

> (Greater than) sign means that rebar on only one face of the section reached yield, and the ultimate capacity will be higher than the value indicated.

Figure 19F-1 ABWR Reactor Building/ Primary Containment (0° - 180° Section View)
(Refer to Figure 1.2-2)

Figure 19F-2 Primary Containment Configuration
(Refer to Figure 6.2-26)

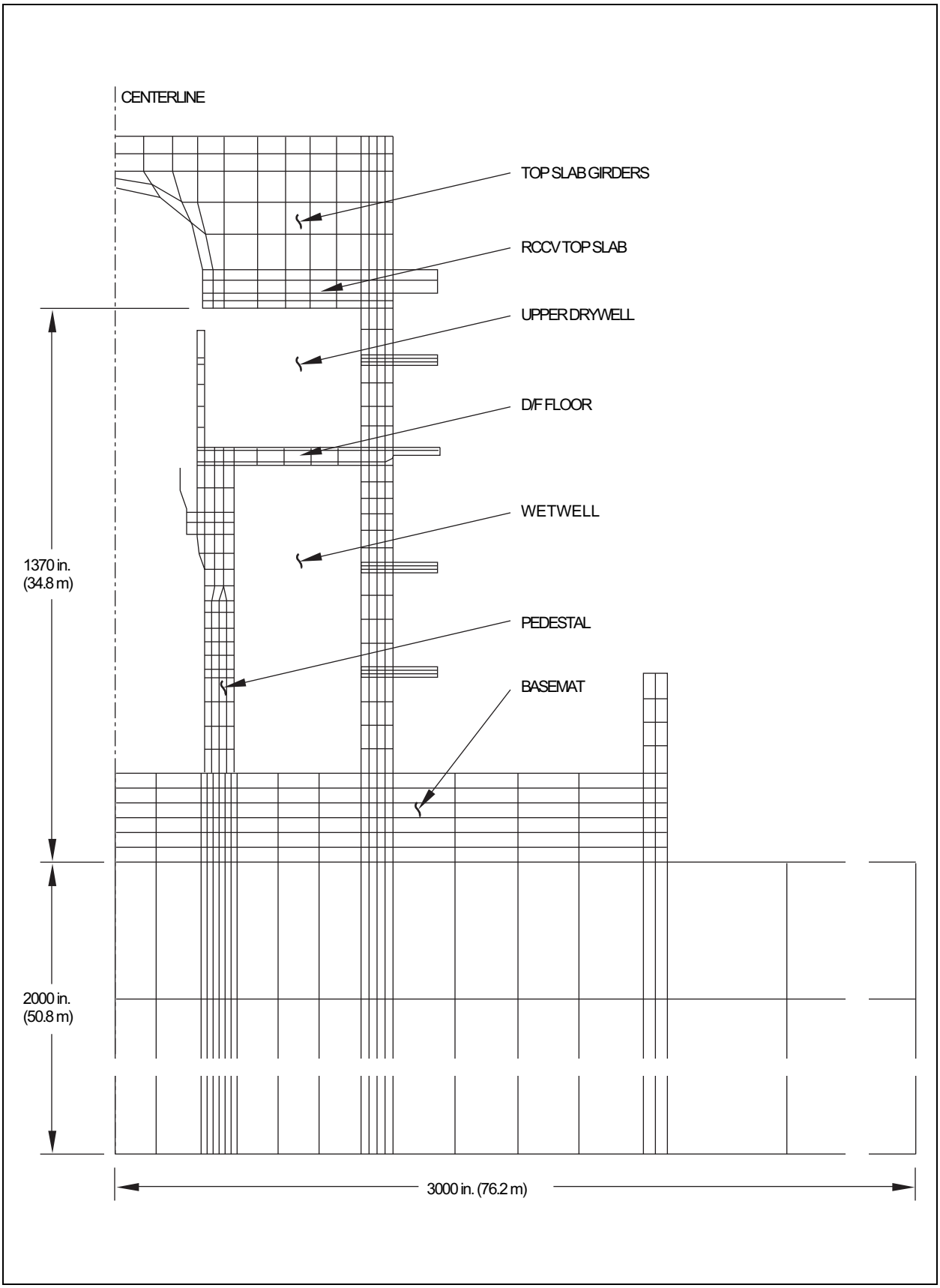

Figure 19F-3 FINEL Model

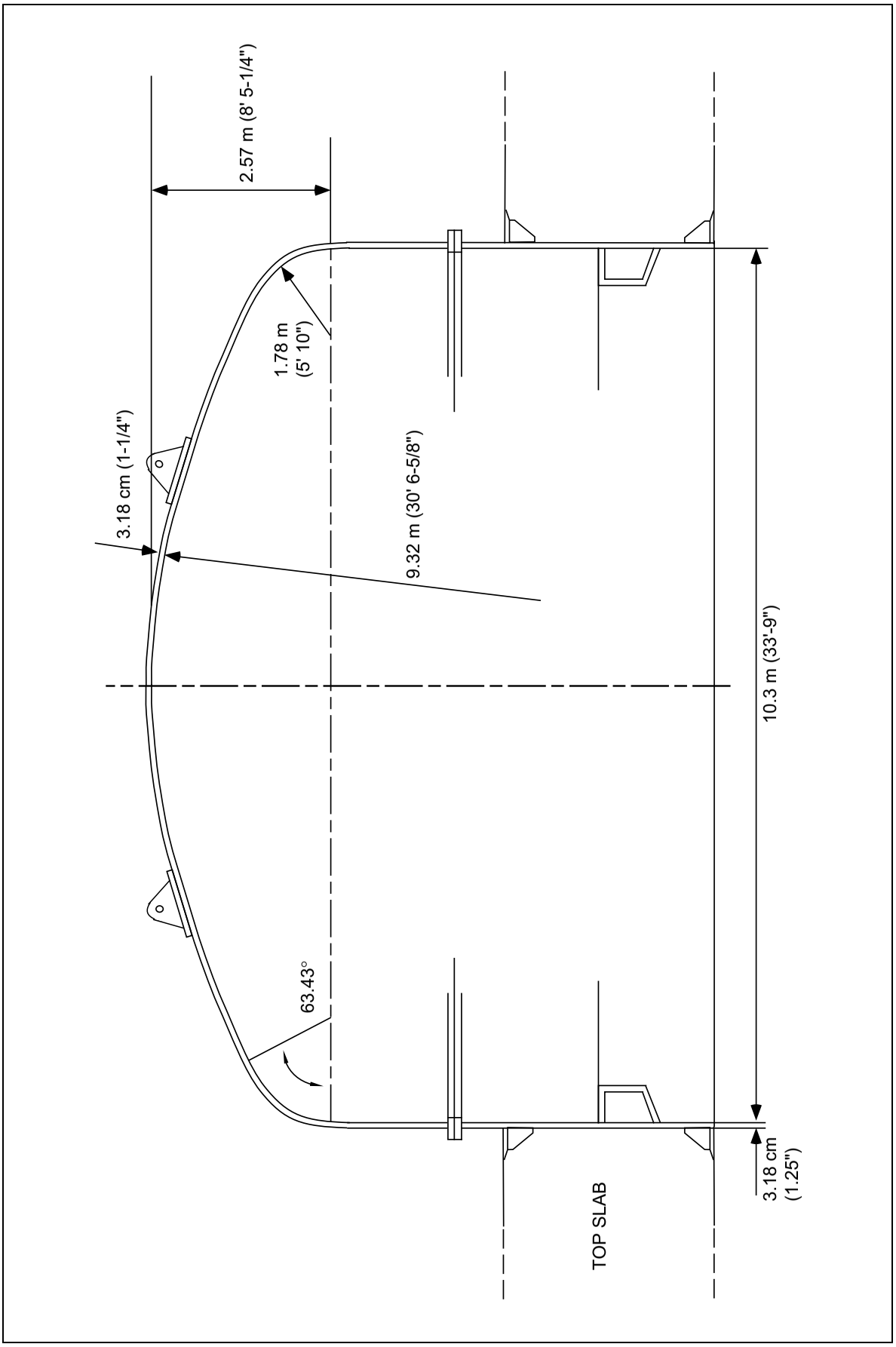

Figure 19F-4 Drywell Head

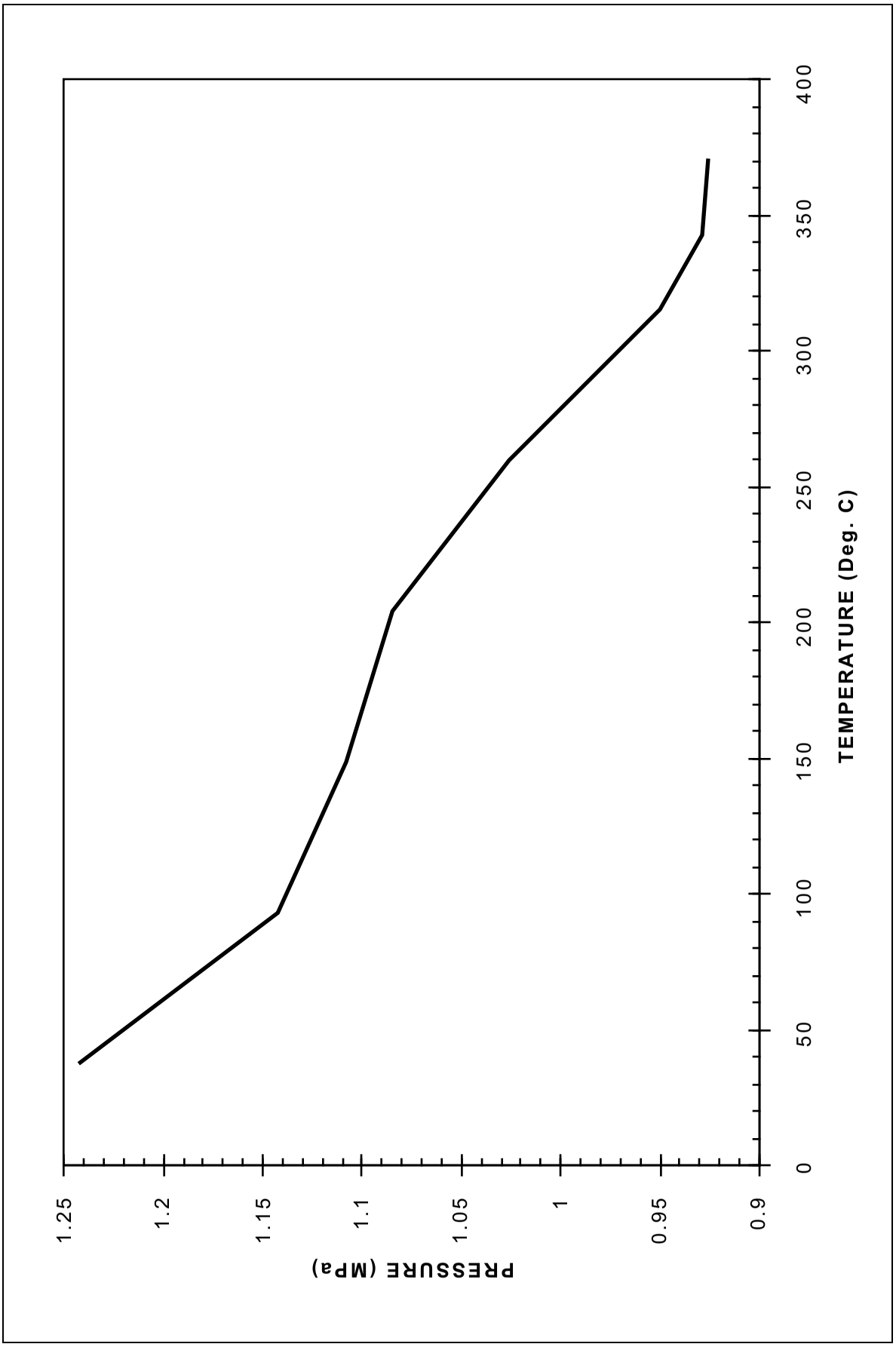

Figure 19F-5 Drywell Head Pressure Capability vs Temperature

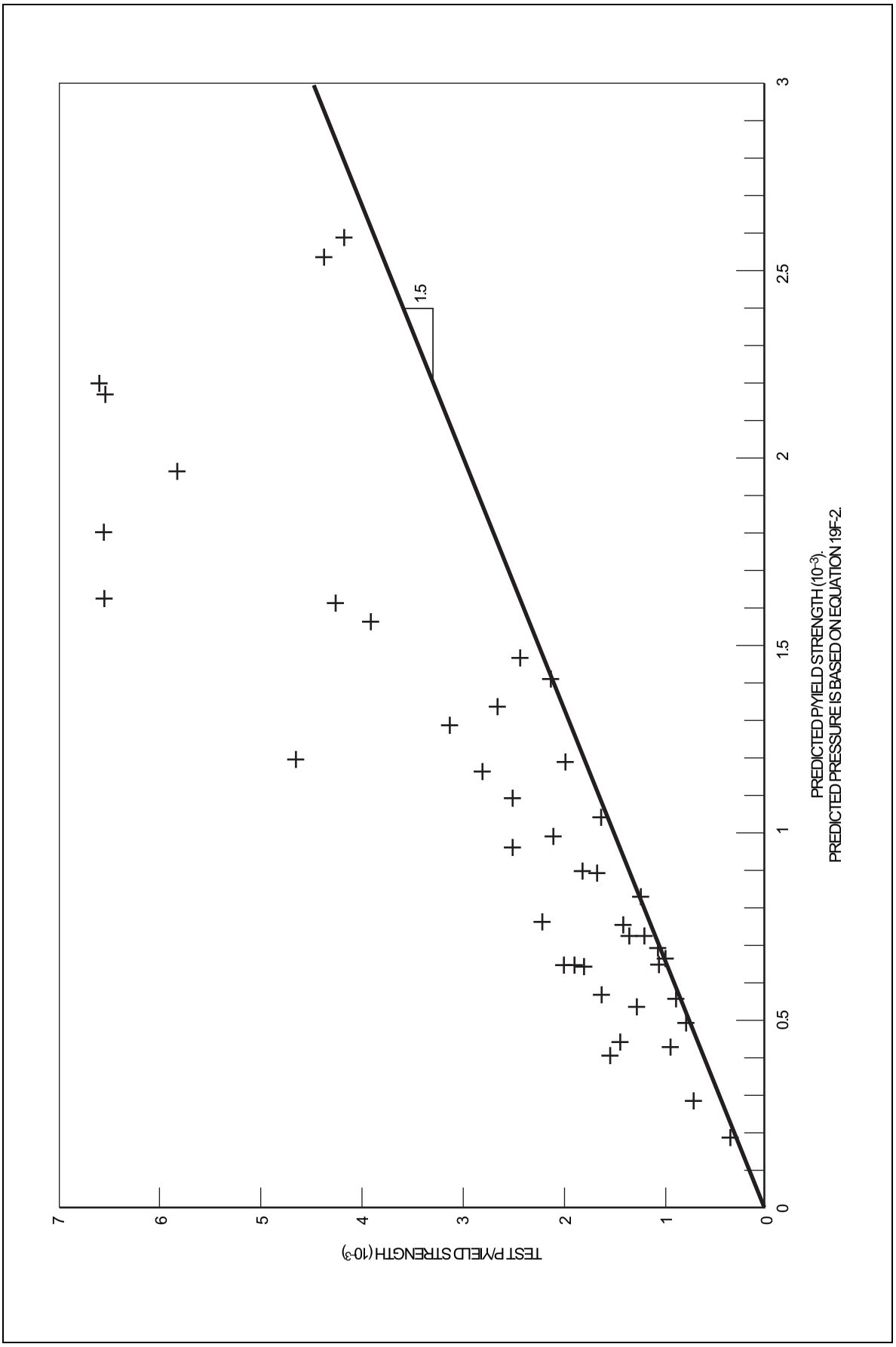

Figure 19F-6 Torispherical Head Buckling Test Data

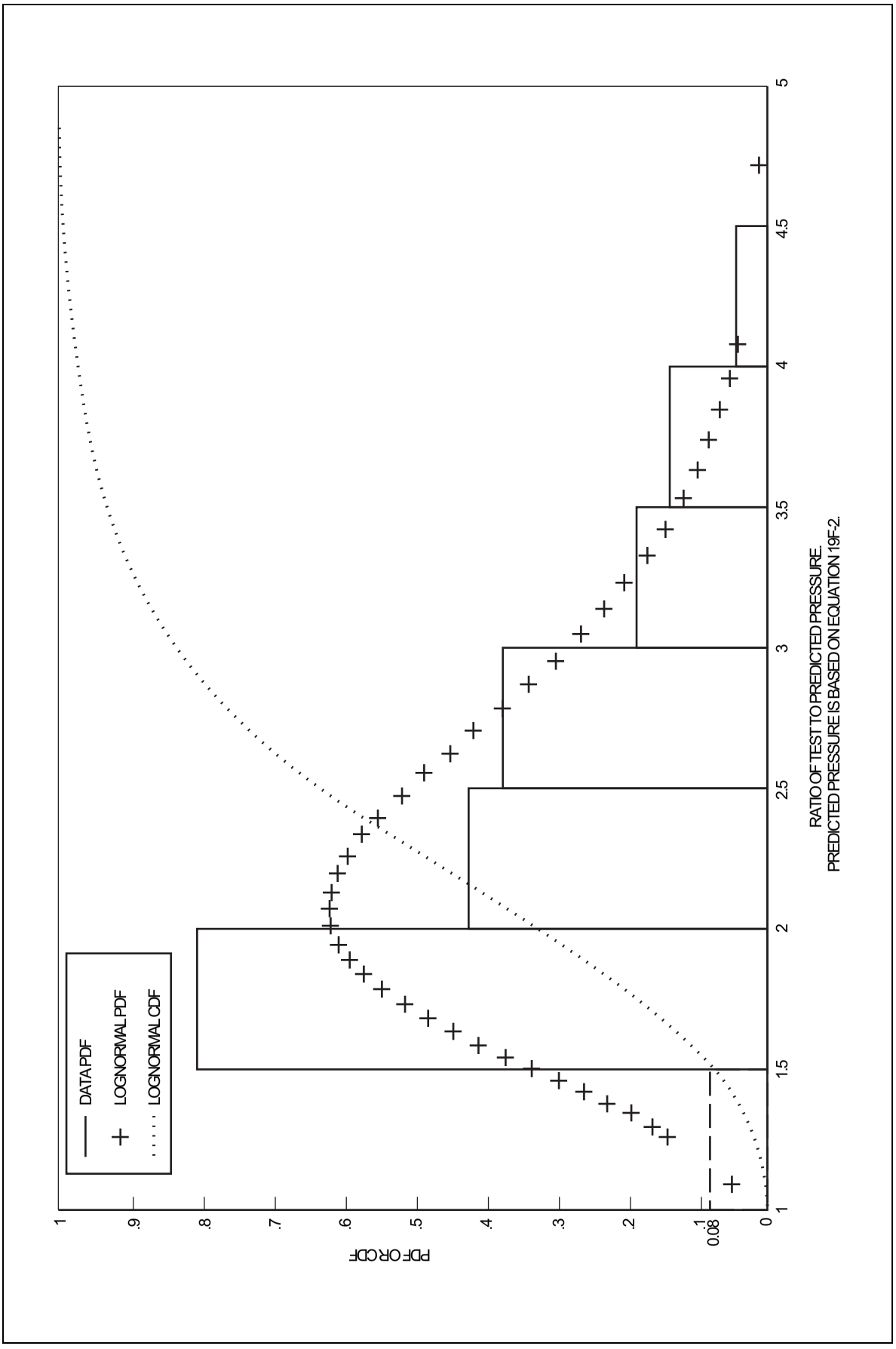

Figure 19F-7 Torispherical Head Buckling Test Data Statistical Distribution

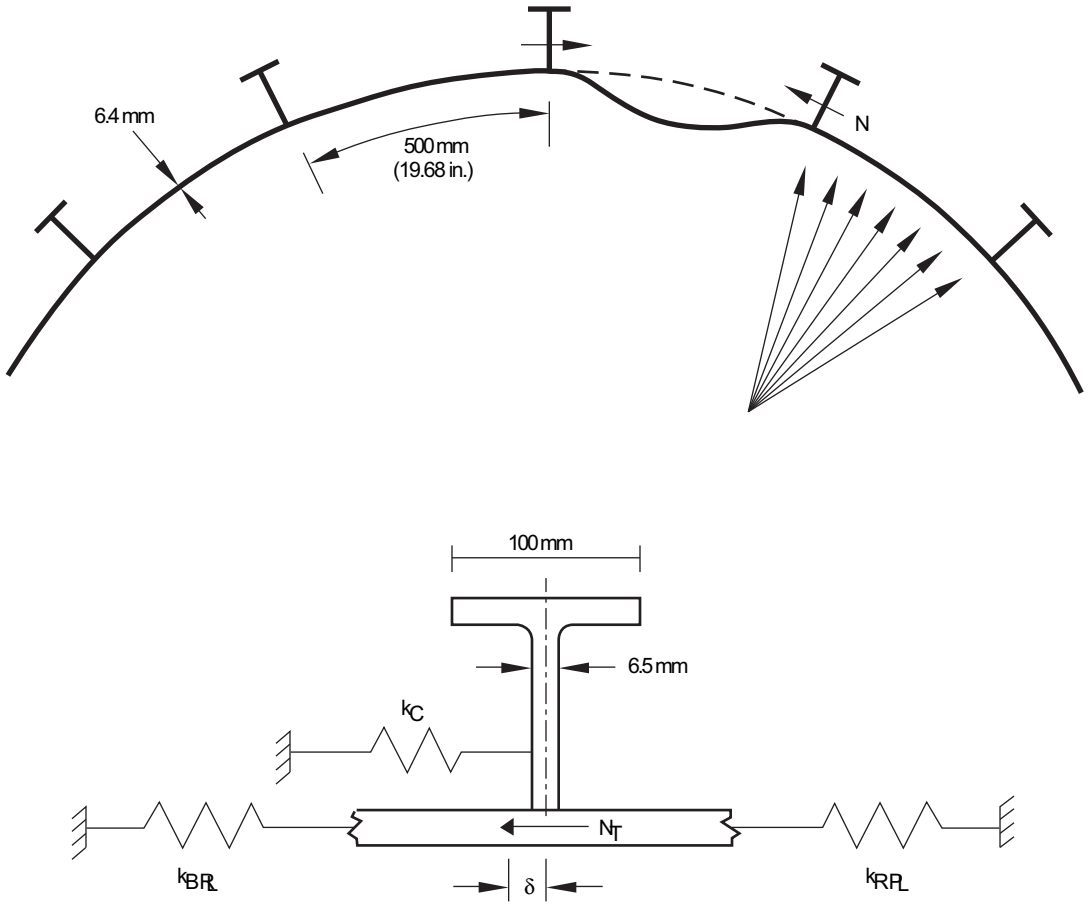

Figure 19F-8 Containment Liner Buckling

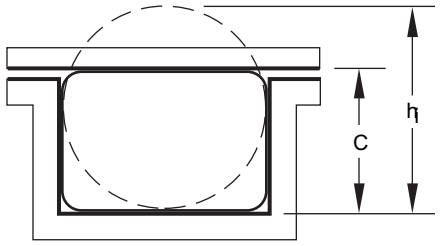

$S_q = (h_i - C)/h_i$

WHERE

h_i = INITIAL SEAL HEIGHT

C = COMPRESSED SEAL HEIGHT IN NORMAL OPERATIONS

Figure 19F-9 Definition of Squeeze for Seals